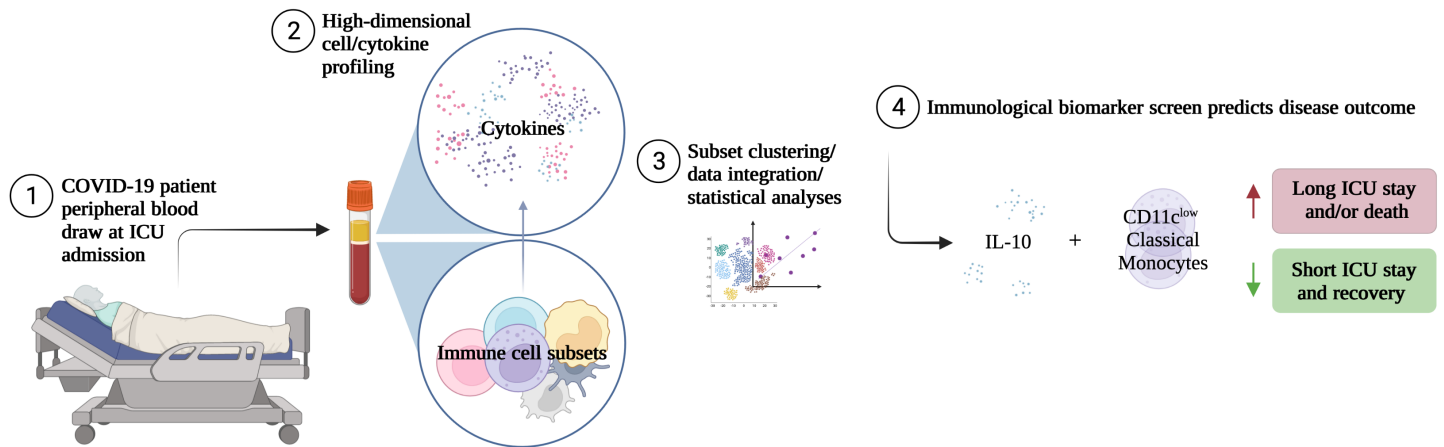


Graphical abstract



Prognostic peripheral blood biomarkers at ICU admission predict COVID-19 clinical outcomes

Melina Messing¹, Mypinder S. Sekhon², Michael R. Hughes¹, Sophie Stukas³, Ryan L. Hoiland⁴, Jennifer Cooper³, Nyra Ahmed³, Mark Hamer¹, Yicong Li¹, Samuel B. Shin¹, Lin Wei Tung¹, Cheryl Wellington³, Don D. Sin^{2,5}, *Kevin B. Leslie¹ and *Kelly M. McNagny¹

¹ The Biomedical Research Centre, Dept of Biomedical Engineering, University of British Columbia, Vancouver, BC, Canada.

² UBC Department of Medicine (Division of Respiriology), Vancouver, BC, Canada.

³ UBC Department of Pathology and Laboratory Medicine, Vancouver, BC, Canada.

⁴ UBC Department of Anesthesiology, Pharmacology, and Therapeutics, Vancouver, BC, Canada

⁵ The University of British Columbia (UBC) Centre for Heart Lung Innovation (HLI), St Paul's Hospital, Vancouver, BC, Canada.

*Corresponding Authors:

Dr. Kelly M. McNagny
Biomedical Research Centre
University of British Columbia
2222 Health Sciences Mall
Vancouver, B.C. CANADA
Ph: 604 822 7824
kelly@brc.ubc.ca

Dr. Kevin B Leslie
Biomedical Research Centre
University of British Columbia
2222 Health Sciences Mall
Vancouver, B.C. CANADA
cytokine86@gmail.com

1 **Abstract**

2 The COVID-19 pandemic continues to challenge the capacities of hospital ICUs which currently
3 lack the ability to identify prospectively those patients who may require extended management. In
4 this study of 90 ICU COVID-19 patients, we used multiplexed cytokine evaluation and, on 42 of
5 these patients (binned into Initial and Replication Cohorts), CyTOF-based deep
6 immunophenotyping. This revealed blood prognostic biomarkers that, at time of ICU admission,
7 prospectively distinguish, with 91% sensitivity and 91% specificity, patients who will
8 subsequently die or have long ICU stays (≥ 6 days) from those who will have short-stays (< 6
9 days). This is achieved through a tiered evaluation of serum IL-10 and targeted
10 immunophenotyping of monocyte subsets (specifically, CD11c^{low} classical monocytes) through
11 statistical approaches. We have distilled this down to a prognostic test that could prove useful in
12 guiding clinical resource allocation, treatment regimens and assessment of new therapeutic
13 interventions.

14 **MAIN**

15 COVID-19 continues to overwhelm effective health care delivery in most parts of the world due
16 to challenges in achieving sufficiently high vaccination rates, vaccine hesitancy and the emergence
17 of more virulent viral variants for which current vaccines offer more modest protection. Thus,
18 waves of rapid outbreaks continue to threaten ICU capacities^{1,2}.

19

20 Individual patient responses to infection by the SARS-CoV-2 virus can vary dramatically ranging
21 from asymptomatic or mild flu-like symptoms to much more severe symptoms including acute
22 respiratory distress syndrome (ARDS) and death^{3,4}. Individual patient outcomes are remarkably
23 challenging to predict but severe disease has been broadly linked to advanced age, obesity,
24 underlying comorbidities and secondary infections^{5,6,7,8,9,10}. Neither symptoms nor conventional
25 clinical measurements (serum C-reactive protein (CRP), blood D-dimers etc.) have sufficient
26 prognostic power and thus approved interventions for severe COVID-19 (including systemic
27 corticosteroids and tocilizumab) are administered broadly as clinicians lack the ability to identify
28 accurately patients at risk of long-term complications and death^{11,12,13,14,15}. Immunologically,
29 “severe” patients have been reported to exhibit lymphopenia, neutrophilia, accumulation of lung
30 monocytes, emergency myelopoiesis, and substantial changes in serum cytokine and chemokine
31 profiles likely reflecting a cytokine storm as the result of a delayed, but exuberant, immune
32 response to infection^{16,17,18,19,20,21,22,23}. The latter has been of particular interest for the development
33 of prognostic tools but while some markers have proven useful in measuring the severity of active
34 COVID-19, to date, they have lacked the necessary statistical power to prospectively predict the
35 likelihood of incipient severe disease^{24,25,26,27,28,29,30,31}. For example, serum IL-6 (alone, or together
36 with other inflammatory markers) has most consistently been linked to severe active disease and,

37 by some groups, was shown to predict the need for subsequent mechanical ventilation as well as
38 survival^{32,33,34,35,36}. In contrast, other studies have struggled to link tightly IL-6 (or TNF α , IFN γ or
39 GM-CSF) to an elevated risk of severe disease and instead have proposed various combinations of
40 serum levels of CCL5, IL-1RA and IL-10, EN-RAGE, TNFSF14 and oncostatin M as indicators
41 of incipient severe disease and, in some cases predictors, of disease severity^{37,38,39}. While,
42 individually, these studies show several biomarkers capable of triaging patients, these inconsistent
43 and sometimes contradictory results highlight the need for biomarkers with robust statistical power
44 to be clinically useful.

45
46 Studies focused on cellular changes have linked a decreased frequency of monocytes (and, more
47 variably, alterations in the frequency of natural killer cells (NK), plasmacytoid dendritic cells
48 (pDC), type-2 conventional dendritic cells (DC2), mucosal associated invariant T (MAIT) cells
49 and other lineages) with active severe disease and poor outcomes^{17,19,34,40,41,42,43,44}. While these
50 global cellular profiling efforts provide important insights into the immune response to SARS-
51 CoV-2 infection, they have yet to be translated into prognostic tools to assist with individualized
52 care.

53
54 Here we focused on the development of an immunological biomarker screen that, at ICU admission
55 for COVID-19, predicts length of ICU stay or death. Strikingly, we find that, at ICU admission,
56 measurements of serum IL-10 and simple monocyte subset surface signatures, specifically,
57 CD11c^{low} classical monocytes, can predict with 91% sensitivity and 91% specificity patients who
58 will either die or have a longer stay in ICU. We offer these biomarkers as a model clinical

59 laboratory test with future potential in gaining insights into variable responses to SARS-CoV-2
60 infection.

61

62 **Results**

63 **COVID-19 patient group selection and optimization of high dimensional immune profiling**

64 To identify potential prognostic markers of COVID-19, we collected PBMCs from 8 healthy
65 controls and, within the first 48 hours of ICU admission, serum samples from 90 ICU COVID-19
66 patients (the “Cytokine Cohort”) admitted during the “second wave” of COVID-19 (November,
67 2020–February, 2021) together with serial serum samples across different timepoints during the
68 course of their ICU admission. PBMCs collected from 14 of these 90 ICU COVID-19 patients (the
69 “Initial Cohort”) were analyzed by mass cytometry (CyTOF) with a training set of 35 monoclonal
70 antibodies (Supplementary Table 1) designed to detect broad shifts in levels of normal PBMC
71 lineages as well as their activation status, and the possible mobilization of tissue resident innate
72 immune cells and bone marrow progenitors into peripheral blood. Based on these data we
73 developed a refined, second-generation, 38-antibody CyTOF panel (Supplementary Table 1),
74 which was used on PBMCs collected from a further 28 of the 90 ICU COVID-19 patients (the
75 “Replication Cohort”). Data from the Replication Cohort were used to validate observations from
76 the Initial Cohort on early alterations in immune responses that could effectively differentiate
77 patients likely to recover after a short ICU stay from those who would either die or have prolonged
78 stays in ICU. The ICU admission sera from all patients in the Cytokine Cohort (which includes all
79 patients in the Initial Cohort and the Replication Cohort) were analyzed for levels of four
80 cytokines: IL-1 β , IL-6, IL-10 and TNF α (Fig. 1a, b).

81

82 Clinical and demographic details of all patients and healthy controls are presented in Table 1 and
83 include age, sex, body mass index (BMI), requirement for ventilation during admission and ICU
84 admission levels of serum CRP, blood D-dimer levels, and white blood cell counts along with their

85 differentials. The average age of the ICU patients was 63.5 years with a 2-to-1 bias towards male
86 patients, consistent with previous patient demographic reports linking more severe COVID-19
87 with older male patients⁴⁵. Table 1 also bins patients into two clinical outcome groups of “Short-
88 Stay” and “Long-Stay/Died” based on the length of time in the ICU and survival: “Short-Stay”
89 patients are classified as those spending < 6 days in the ICU and were survivors, while “Long-
90 Stay/Died” patients are defined as patients who spent 6 or more days in the ICU or died during
91 their stay in ICU. The choice of 6 days as the cut-off was based upon iterative empirical analyses
92 of immune data that divided, with greatest statistical significance (by p-value), patients into two
93 sub-groups with distinct clinical outcomes (Fig. 1a, c).

94
95 Importantly, we found no significant differences between the two clinical outcome groups with
96 respect to mean age, BMI, blood clotting parameters (D-dimer levels) or serum CRP levels (Fig.
97 1d, e). At admission, the mean total PMN counts were significantly increased in the Long-
98 Stay/Died group compared to the healthy controls ($p < 0.0001$) and compared to the Short-Stay
99 group ($p = 0.025$) (Fig. 1f). In our separate analyses of just the Initial Cohort and Replication
100 Cohorts, however, differences in PMN counts were not statistically significant and thus we did not
101 consider this measurement as a useful prognostic biomarker of clinical outcomes in the context of
102 smaller cohort numbers. PBMC counts were also not significantly changed between healthy
103 controls and patients or between our two clinical outcome groups (Fig. 1f). Thus, while these
104 routine clinical tests follow a broad spectrum of parameters including inflammation, coagulopathy,
105 hypo-immunity and autoimmunity, none consistently proves prognostic in identifying patients
106 who would require an extended stay in ICU or die. Accordingly, we conducted more detailed

107 immunological examinations focused on a single, specific COVID-19-associated process, namely
108 inflammation.

109

110 **Serum cytokine analyses as prognostic screens for predicting clinical outcome**

111 We began by examining serum levels of IL-1 β , IL-6, IL-10 and TNF α at ICU admission in all
112 serum samples from our Cytokine Cohort of 90 COVID-19 patients. Strikingly, we found that the
113 mean ICU admission levels of serum IL-10 ($p = 0.004$) and TNF α ($p = 0.0005$) were significantly
114 elevated in the Long-Stay/Died group relative to the Short-Stay group (Fig. 1g). In the Cytokine
115 Cohort, 43% (39/90) of patients had serum ICU admission levels of IL-10 levels ≥ 15 pg/ml and
116 79% (31/39) of these patients fell into the Long-Stay/Died group. Similarly, 42% (38/90) of
117 patients in the Cytokine Cohort had serum ICU admission levels of TNF α ≥ 10 pg/ml and 79%
118 (30/38) of these patients were members of the Long-Stay/Died group. Interestingly, serum IL-10
119 and TNF α only showed a weak correlation with each other (Pearson correlation coefficient $R^2 =$
120 0.12) suggesting that each may represent a different aspect or chronology of the inflammatory
121 process.

122

123 Given the clear prognostic value of ICU *admission levels* of TNF α and IL-10, we also examined
124 the subsequent mean maximum serum cytokine levels in *post admission* samples from patients in
125 the Short-Stay and the Long-Stay/Died groups and found an even more significant difference
126 between the two groups for both serum TNF α ($p < 0.0001$) and serum IL-10 ($p = 0.0009$) (Fig.
127 1h). Intriguingly, many patients in the Long-Stay/Died group who demonstrated modest admission
128 levels of serum IL-10 and TNF α subsequently developed high levels during their stay in ICU,

129 further reinforcing the importance of these two cytokines as predictive measures of patient
130 outcomes and monitoring the trajectory of disease.

131
132 While admission levels of serum IL-6 were also significantly different between the two clinical
133 groups ($p = 0.007$) (Fig. 1i), we excluded this cytokine from further analyses due to the potential
134 confounding effects of anti-IL-6 receptor antibody (tocilizumab) treatments, which has routinely
135 been administered to COVID-19 patients in British Columbia during ICU admission since
136 February 2021 and such treatments could complicate the interpretation of our results. Finally, there
137 were no significant differences between the two clinical outcome groups with respect to mean
138 serum IL-1 β levels at ICU admission ($p = 0.205$) and thus this cytokine was also not analyzed
139 further (Fig. 1i). In summary, we found that ICU admission levels of serum IL-10 and TNF α were
140 useful and statistically powerful prognostic markers for clinical outcomes in severe COVID-19.

141

142 **Major PBMC subsets fail to distinguish Short-Stay from Long-Stay/Died patients**

143 We examined whether parallel CyTOF analyses of peripheral immune cells sampled at the time of
144 ICU admission could reveal additional prognostic biomarkers that identify patients in the Long-
145 Stay/Died group, particularly among those that had serum IL-10 levels <15pg/ml and/or serum
146 TNF α levels <10pg/ml. PBMC samples were available for 42/90 of the Cytokine Cohort patients,
147 and these 42 samples were divided into an Initial Cohort (14 samples) and a Replication Cohort
148 (28 samples).

149
150 Using a 35-marker CyTOF panel on the Initial Cohort (Supplemental Figure 1) and a 38-marker
151 CyTOF panel on the Replication Cohort (Fig 1.), we saw no differences between the Short-Stay

152 patients and Long-Stay/Died patients with respect to major peripheral blood immune populations.
153 The more-focussed and larger 38-marker CyTOF panel, used to analyze immune cell subsets in
154 the Replication Cohort, permitted clear identification of broad blood cell lineages (B, T, NK, and
155 myelomonocytic) as well as major subsets within each cell lineage leading to 41 distinct cell subset
156 clusters based on the variable expression of these cell-surface markers (Fig. 2a-c). While these
157 analyses of the Replication Cohort samples and the Initial Cohort samples confirmed previous
158 reports^{5,46} of general lymphopenia in COVID-19 patients relative to healthy controls with respect
159 to both total CD4 T cells and total CD8 T cells, these markers failed to discriminate between the
160 Short-Stay and Long-Stay/Died patient groups. Also consistent with previous reports, we observed
161 no significant differences in total B cells in COVID-19 patients compared to healthy controls or
162 between the two clinical outcome groups (Fig. 2d). Although mean total NK cells, MAIT cells, $\gamma\delta$
163 T cells, DC2/3 and pDC were depleted in COVID-19 patients relative to healthy controls these,
164 too, failed to distinguish the Short-Stay group from the Long-Stay/Died group (Fig. 2e). Finally,
165 while mean total monocytes and stem cell levels were significantly increased in COVID-19
166 patients relative to healthy controls they failed, individually, to distinguish the Short-Stay from the
167 Long-Stay/Died patient groups (Fig. 2f). In summary, broad immune subset analyses were
168 insufficient to predict COVID-19 patient clinical outcomes with respect to the length of stay in
169 ICU and/or death in either the Initial Cohort or the Replication Cohort. We, therefore, performed
170 more detailed analyses of immune cell subsets within these broad cell categories to identify more
171 subtle potential differences between the two clinical outcome groups that could assist in the
172 prospective identification of Long-Stay/Died patients.

173

174 **Levels of a distinct monocyte subset at the time of ICU admission predicts subsequent clinical**
175 **outcome**

176 To reveal a larger diversity of specific immune cell subsets we performed more focused cluster
177 analyses on patient PBMC samples from the Initial Cohort and the Replication Cohort after pre-
178 gating for selected major cellular subsets. To restrict the clustering to the myelomonocytic
179 compartment we performed gated analyses on GM-CSFR⁺(CD116⁺) CD19⁻ CD3⁻ cells (Fig. 3a)
180 and restricted clustering to shared marker channels to enable direct comparison between the Initial
181 and the Replication cohorts. These analyses did not reveal subsets that separated Short-Stay from
182 Long-Stay/Died patients with respect to absolute cell counts. To focus more specifically on the
183 monocytic subsets as well as to simplify the cluster analyses, after pre-gating on CD116⁺ CD19-
184 CD3- cells, we restricted the marker channels selected for clustering to a set of 7 markers useful
185 in defining monocytic subsets (CD45, CD14, CD16, CD11c, HLA-DR, CD123, CD56, see Figs.
186 3b,c). Interestingly, this strategy revealed a CD11c^{low} classical monocytic subset (CD45⁺ CD116⁺
187 CD3ε⁻ CD11c^{low} HLA-DR⁺ CD14⁺ CD16^{-/low} CD123^{-/low}) that, in both the Initial and the
188 Replication Cohorts, was consistently enriched in COVID-19 patients relative to healthy controls
189 (p = 0.001, Replication Cohort) and was preferentially enriched in the Long-Stay/Died group
190 relative to the Short-Stay group (p = 0.019, Replication Cohort) (Fig. 3d). The prognostic value of
191 the CD11c^{low} classical monocytic marker was restricted to this subset of classical monocytes in
192 both the Initial and Replication Cohorts and did not reflect underlying changes of total classical
193 monocytes which were unchanged in the two clinical outcome groups (Fig. 3e). Moreover, for
194 both Initial and Replication Cohorts, total intermediate monocytes (CD14⁺ CD16^{int}) and total non-
195 classical monocytes (CD14^{low} CD16⁺), as well as observed subpopulations of these types of
196 monocytes, did not prove useful prognostically (Fig. 3f). Focussing the analyses further on

197 classical monocytes, we found that a three-marker gating strategy was sufficient to identify the
198 CD11c^{low} classical monocyte population identified by our multi-dimensional analyses (shown here
199 for one representative sample from each group in the Replication Cohort, where intensity is
200 proportional to relative frequency of cells) (Fig. 3g). Thus, the prognostically useful biomarker of
201 CD11c^{low} classical monocytes was detectable in two dimensions in both the Initial and the
202 Replication Cohorts using antibodies to a small set of cell-surface markers.

203
204 Because lymphopenia has been a consistent feature of severe COVID-19 and T cell subset
205 alterations have been described, we performed similar in-depth analyses of the T cell
206 compartments by gating on CD3⁺ cells prior to clustering. Consistent with our analyses of major
207 subsets in the previous section, we were able to confirm and extend our and other groups' findings
208 that more subtle T cell subsets are significantly depleted in patients relative to healthy controls
209 including subsets in the CD4⁺, CD8⁺, MAIT and $\gamma\delta$ T cell compartments (Supplementary Figure
210 2). However, while we gained valuable insight into the altered T cell response in COVID-19
211 patients, none of these T cell subsets were prognostically useful in separating the Long-Stay/Died
212 patients from the Short-Stay patients.

213

214 **Combined evaluation of immune parameters as a tool to predict clinical outcome**

215 Since deeper analyses of multiple cytokines and cell subsets at ICU admission revealed significant
216 differences between the Long-Stay/Died and Short-Stay groups, we sought to combine these
217 findings to generate a streamlined prognostic tool that could accurately predict whether a patient,
218 newly admitted to ICU, was likely to have a subsequent longer stay in ICU or die. Although both
219 serum TNF α and serum IL-10 were significantly elevated in Long-Stay/Died patients relative to

220 Short-Stay patients in the Cytokine Cohort, using Pearson analyses, the length of stay in ICU
221 correlated more significantly with serum IL-10 levels ($R^2 = 0.48$) and maximum IL-10 levels (R^2
222 $= 0.54$) than with serum levels of TNF α ($R^2 = 0.14$). Thus, we proceeded with serum IL-10, only,
223 as our cytokine-based pre-screen portion of a stepwise integrated prognostic tool. As the first step,
224 using a cut-off value of 15pg/ml for serum IL-10, data from the 90-sample Cytokine Cohort
225 demonstrated a 79% specificity and 55% sensitivity in predicting that a patient newly admitted to
226 ICU would have a longer stay in ICU or die (Fig. 4g). This prognostic specificity of 79% is
227 somewhat comparable with that seen in the smaller subsets of the Cytokine Cohort, namely the
228 14-sample Initial Cohort (86%) and the 28-sample Replication Cohort (100%). Similarly, the
229 prognostic sensitivity of 55% in the Cytokine Cohort is somewhat comparable with that observed
230 in the Initial Cohort (86%) and the Replication Cohort (56%) (Figs. 4a-c,g). The variations in
231 estimates of prognostic sensitivity and specificity between cohorts (the Cytokine Cohort and its
232 two subsets of the Initial Cohort and Replication Cohort), however, likely demonstrate variations
233 that reflect the influences of random patient sampling and, very importantly, cohort size. These
234 results validate serum IL-10 levels as a pre-screen for patients likely to die or to experience a long
235 ICU stay.

236

237 We then explored the utility of combining serum IL-10 levels (with a cut-off value of 15pg/ml)
238 with the levels of CD11c^{low} classical monocytes (with a cut-off value of 2.7×10^7 /ml) as a stepwise
239 integrated diagnostic tool. With this approach, 100% of the Long-Stay/Died patients were correctly
240 identified in the Initial Cohort and 88% of Long-Stay/Died patients were correctly identified in the
241 Replication Cohort, the latter with a specificity of 100% (Figs. 4d,e,g). These analyses of all 42
242 patients in the combined Initial and Replication Cohorts ($n = 42$) allowed us to predict with 91%

243 sensitivity and 91% specificity the clinical outcome of COVID-19 patients newly admitted to ICU
244 with respect to the likelihood of extended stay or death in ICU (Figs. 4f,g). Thus, our results
245 suggest that a simple screen of two biomarkers at the time of ICU admission allows for rapid
246 identification of those patients who are likely to die or require extended ICU care (Fig. 4h) and has
247 clear implications for patient care and health care delivery.

248

249 **Discussion**

250 The goal of the present study was to identify prognostic biomarkers that, at time of ICU admission,
251 could predict subsequent outcome of COVID-19. Such markers are in urgent need and, with further
252 testing and refinement, could serve to triage patients into specific groups for timely and appropriate
253 care while, at the same time, offer insights into the immune-mediated determinants of disease
254 response. Like many previous studies, we found that although severe COVID-19 is linked to broad
255 shifts in peripheral blood immune subsets (increased PMNs and T cell lymphopenia) and increased
256 blood inflammatory markers (CRP, D-dimer, etc.), none of these proved prognostic with respect
257 to subsequent length of ICU stay and/or death. Therefore, we used CyTOF-based PBMC
258 immunophenotyping and serum cytokine analyses on samples drawn at ICU admission to focus
259 our attention on more subtle shifts in inflammatory parameters with a view to identifying
260 prognostic biomarkers. Through iterative empirical analyses of these data, we identified two
261 groups of ICU patients who would subsequently have clinically distinguishable disease outcomes:
262 those who would be discharged from ICU within 6 days and those who would require a longer
263 ICU stay or die. We then used retrospective analyses to generate a simple set of biomarkers that
264 could easily be applied in the clinic to identify, at the time of ICU admission, those patients at
265 greater risk of death or lengthy stay in ICU.

266

267 A high admission level of serum IL-10 ($\geq 15\text{pg/ml}$), alone, was (in a cohort of 90 patients) a
268 singular powerful biomarker that identified patients in the Long Stay/Died group with 79%
269 specificity, though with a lower sensitivity of 55%. Additional high dimensional cell surface
270 protein analyses of 42 patients revealed a simple set of monocyte markers, specifically those
271 identifying CD11c^{low} classical monocytes, that when combined with admission serum IL-10 levels
272 accurately predicted with 91% specificity and 91% sensitivity at the time of ICU admission
273 patients who would subsequently either have a longer stay in ICU or who would die (validated in
274 initial and replication cohorts). Thus, based on the information from our evaluation of 4 serum
275 cytokines and 38 surface markers and validated on two separate clinical cohorts, we have distilled
276 our prognostic screen down to a composite test of one cytokine and one monocyte subset as
277 predictive biomarkers that could be evaluated in most clinical laboratories. Indeed, our
278 demonstration that the cellular biomarker can be detected and visualized in two dimensional
279 analyses (Fig 3f) using limited markers reinforces the likelihood that this biomarker will be
280 detectable using conventional clinical flow cytometry.

281
282 Although individually several of the biomarkers examined here have been investigated previously
283 and described as markers of disease severity, there has been a lack of clear consensus on their
284 prognostic utility in the published literature. For example, both IL-6 and IL-10 emerged early as
285 candidate clinical markers of disease severity, but to our knowledge are not widely used in standard
286 prognostic testing at hospital or ICU admission^{32,33,36,37}. This likely reflects the fact that, used in
287 isolation and without a detailed quantitative evaluation of threshold levels predicting outcome,
288 their presence or absence provides a more superficial indication of current inflammatory status and
289 fails to predict the temporal trajectory of clinical disease (increasing or decreasing severity). This

290 also may explain why anti-IL-6 receptor therapy has shown only limited efficacy as a broad-
291 spectrum therapeutic for severe COVID-19 and fails to reduce overall mortality^{13,47}. Similarly,
292 although corticosteroids have emerged as a standard-of-care for COVID-19 ICU patients and
293 undoubtedly provide improved recovery after infection, they are widely recognized as “double-
294 edged swords”: while they are effective at suppressing excessive inflammation, they also potently
295 suppress adaptive immune responses, potentially reducing viral clearance and increasing
296 susceptibility to secondary infections^{12,48}. With that backdrop, a benefit of the streamlined ICU
297 biomarker panel described here is that it provides a direct prognostic link to patient outcome and
298 may also serve as a biomarker panel for monitoring patient response to therapies.

299
300 In our study, deep immunophenotyping of the myeloid compartment in COVID-19 patients proved
301 pivotal in defining markers to predict patient outcomes. While we saw no significant early changes
302 in total monocyte numbers or total classical monocyte numbers or frequencies, a prognostically
303 useful monocytic subset was contained within these broader subsets which highlights the need for
304 a high-dimensional evaluation to identify subtle, but informative, changes in immune
305 subpopulations that might otherwise have been overlooked. After identification of such subtle
306 biomarkers using high-dimensional analytic technologies, simpler two-dimensional technologies
307 (using limited markers) can then be used to measure the biomarker clinically. It is noteworthy that
308 previous studies have linked both increased peripheral blood monocytes and increased numbers of
309 inflammatory macrophages in the lung to severity of COVID-19^{49,50,51,52}. Other studies reported
310 subtle, monocyte subset-specific changes in severe COVID-19, including dysfunctional pro-
311 inflammatory cytokine production, reduction in HLA-DR transcripts, accumulation of HLA-DR^{low}
312 monocytes and reduction of non-classical monocytes^{16,17,34,38,42}. Further, CD11c^{low} monocytic

313 enrichment has been described in severe COVID-19¹⁷. The data presented here confirm and extend
314 these observations in a manner that facilitates accurate prognostication. They also reveal CD11c^{low}
315 classical monocytes as new target populations for more focused mechanistic studies in future
316 research. While the combination of these two biomarkers certainly provides prognostic
317 information on disease outcome in COVID-19, there is a possible parallel interpretation of the
318 results: since all patients received corticosteroids at the time of admission, the biomarkers
319 described here may actually be identifying those patients who are, in fact, more responsive to
320 corticosteroid therapy. We leave this intriguing possibility for future investigation.

321
322 Although not specifically addressed here, we believe that these prognostic biomarkers provide a
323 roadmap for future studies aimed at guiding and monitoring response to therapy. Such monitoring
324 is particularly important in the context of therapies that have the acknowledged potential of
325 exacerbating clinical disease if given in a temporally inappropriate manner in the COVID-19 cycle
326 of stimulation and progression to clearance and resolution. While we have focused here on the
327 utility of these markers at the time of ICU admission it is possible that these may prove even more
328 valuable as temporal monitoring tools for revealing disease trajectory on this continuum and
329 responses to therapeutic intervention.

330

331 **Methods**

332 ***Patients, controls, and clinical information***

333 This study was approved by the University of British Columbia Clinical Research Ethics board
334 (H20-00685) and patient blood was collected at St. Paul's Hospital and Vancouver General
335 Hospital in Vancouver, BC. All COVID-19 patients had a positive nasal or tracheal real time
336 reverse transcription polymerase chain reaction (RT-PCR) SARS-CoV-2 test. To avoid
337 unnecessary virus exposure, patient blood was collected in concert with routine care. Patient
338 samples (n = 90) were collected within 48 hours of ICU admission between November 2020 and
339 February 2021. Patient demographics and clinical information are listed in table 1. Patient samples
340 were transported to the main campus of the University of British Columbia for further processing.
341 Healthy control blood samples (n = 8) were collected from age-matched volunteers who showed
342 no COVID-19 symptoms or other illnesses and that had no history of COVID-19.

343

344 ***Specimen collection and isolation***

345 Blood designated for peripheral blood mononuclear cell (PBMC) analysis was collected into
346 citrate coated BD Vacutainer™ Glass Mononuclear Cell Preparation (CPT) tubes and PBMCs
347 were isolated within four hours following collection according to manufacturer guidelines. Red
348 blood cell lysis was performed with ACK lysing buffer (Gibco) for 10 minutes. Isolated PBMCs
349 were frozen in fetal bovine serum (Gibco) with 10% dimethyl sulfoxide and stored in liquid
350 nitrogen. Blood designated for serum analysis was collected into BD Vacutainer™ Serum
351 Separation Tubes (SST) and allowed to clot for at least 30 minutes prior to centrifugation at 1200
352 rcf for 10 minutes and serum collection and storage at -80 °C.

353

354 ***Antibody staining and CyTOF data collection***

355 Frozen PBMCs were thawed at 37 °C and washed with RPMI 1640 containing 10% FBS and 25U
356 nuclease (Thermo Fisher Scientific). Between 1- 4 x 10⁶ cells per sample were used for antibody
357 staining. Prior to fixation, all centrifugation steps were performed at 500 rcf and 4 °C. All reagent
358 dilutions were prepared according to manufacturer instructions unless stated otherwise. For
359 live/dead cell analysis, PBMCs were stained with Cell-ID™ Intercalator-Rh (Fluidigm) for 15
360 minutes at 37 °C and washed with MaxPar® MCSB. Prior to surface staining, cells were incubated
361 with human TruStain FcX™ (Biolegend) for 15 minutes at 4 °C and stained with a surface antibody
362 cocktail for 30 minutes at RT (see Supplemental Table 2 for complete list of antibodies). The MR1-
363 5-OP-RU tetramer was incubated together with the antibody cocktail. After incubation, the cells
364 were washed and incubated for 30 minutes at RT with the secondary anti-APC antibody. Prior to
365 fixation and nuclear staining, PBMCs were washed with MaxPar® MCSB and incubated in
366 MaxPar® Fix and Perm Buffer (Fluidigm) and Cell-ID™ Intercalator-IR (Fluidigm) for 1 hour.
367 Post fix, all centrifugation steps were performed at 900 rcf and 4 °C. To prepare for CyTOF
368 acquisition, PBMCs were washed with MilliQ water and resuspended in EQ™ Four Element
369 Calibration Beads (Fluidigm). Samples were acquired with a CyTOF®2 mass cytometer. An
370 average of 400,000 events were collected for each sample at a flow rate of 45µl/min.

371

372 ***Cytokine data collection***

373 Serum cytokines IL-6, IL-10, TNFα and IL-1β were quantified using the Simoa HD-1 platform
374 from Quanterix (Billerica, MA) according to manufacturing guidelines and as specified by Stukas
375 *et. al.*⁵³.

376

377 ***Data processing***

378 All data files were normalized (<https://github.com/nolanlab/bead-normalization>) and events of
379 interest were manually gated with the FlowJo gating software (BD Biosciences). Dimensionality
380 reduction and clustering were performed with Uniform Manifold Approximation and Projection
381 (UMAP) and Rphenograph respectively, as provided in the bioconductor package Cytofkit
382 (<https://github.com/JinmiaoChenLab/cytofkit2>). The input files were equally down sampled and
383 cytofAsinh was used as the transformation method. The Rphenograph k was set to the default of
384 30. The dimensionality reduction and clustering were both performed on the entire data set as well
385 as separately on manually pre-gated populations. Populations were identified manually based on
386 marker expression (e.g., T cells were identified based on expression of CD3, CD4 or CD8).

387

388 ***Statistical analysis and figures***

389 Sample size and statistical tests are indicated in figure legends and all graphs and statistical tests
390 were generated using GraphPad Prism (GraphPad Software, La Jolla California, USA). A test was
391 considered statistically significant at a probability of $< 5\%$ ($p < 0.05$) and we did not assume a
392 Gaussian distribution. UMAP plots and heatmaps were exported from Cytofkit and experimental
393 outline figures, including the graphical abstract were created using BioRender.com. Figures were
394 assembled in Microsoft PowerPoint.

395

396 **Acknowledgements**

397 This study was supported by the St. Paul's Foundation. We thank the healthcare teams from St.
398 Paul's Hospital and Vancouver General Hospital as well as the technical support from the
399 Biomedical Research Centre core facility members Michael Williams (AbLab) and Andy Johnson
400 (ubcFLOW cytometry). We acknowledge that the following reagent was obtained through the NIH
401 Tetramer Core Facility: APC coupled MR1-5-OP-RU tetramer. Finally, we thank Jeff Biernaskie
402 and Bryan Yip at the University of Calgary for helpful discussions and generous seed funding from
403 the Thistledown Foundation.

404

405 **Contributions**

406 M.M. was responsible for patient sample processing and mass cytometry experiments. K.M.M.,
407 K.B.L. and M.M. were responsible for study design, data analyses, interpretation, and manuscript
408 preparation. M.S.S., R.L.H. and D.D.S. provided patient samples and clinical information. M.R.H.
409 managed ethics approvals and assisted with data analyses and interpretation. S.S., C.W., J.C. and
410 N.A. processed serum samples and acquired serum data. S.B.S., Y.L., L.W.T. and M.H. provided
411 technical assistance for patient sample processing and mass cytometry data collection and
412 processing. All authors contributed to editing the manuscript.

References

1. Cevik, M., Kuppalli, K., Kindrachuk, J. & Peiris, M. Virology, transmission, and pathogenesis of SARS-CoV-2. *BMJ* **371**, (2020).
2. Wiersinga, W. J., Rhodes, A., Cheng, A. C., Peacock, S. J. & Prescott, H. C. Pathophysiology, Transmission, Diagnosis, and Treatment of Coronavirus Disease 2019 (COVID-19): A Review. *JAMA* **324**, 782–793 (2020).
3. Wang, D. *et al.* Clinical Characteristics of 138 Hospitalized Patients With 2019 Novel Coronavirus-Infected Pneumonia in Wuhan, China. *JAMA* **323**, 1061–1069 (2020).
4. Matthay, M. A. *et al.* Acute respiratory distress syndrome. *Nat. Rev. Dis. Prim.* **5**, (2019).
5. Huang, C. *et al.* Clinical features of patients infected with 2019 novel coronavirus in Wuhan, China. *Lancet* **395**, 497–506 (2020).
6. Chen, G. *et al.* Clinical and immunological features of severe and moderate coronavirus disease 2019. *J. Clin. Invest.* **130**, 2620–2629 (2020).
7. Lavezzo, E. *et al.* Suppression of a SARS-CoV-2 outbreak in the Italian municipality of Vo'. *Nat.* **2020 5847821** **584**, 425–429 (2020).
8. Carotti, M. *et al.* Chest CT features of coronavirus disease 2019 (COVID-19) pneumonia: key points for radiologists. *Radiol. Med.* **125**, 1 (2020).
9. Parekh, M., Donuru, A., Balasubramanya, R. & Kapur, S. Review of the Chest CT Differential Diagnosis of Ground-Glass Opacities in the COVID Era. <https://doi.org/10.1148/radiol.2020202504> **297**, E289–E302 (2020).
10. Feng, Z. *et al.* Early prediction of disease progression in COVID-19 pneumonia patients with chest CT and clinical characteristics. *Nat. Commun.* **11**, (2020).
11. Chen, J. S. *et al.* Nonsteroidal Anti-inflammatory Drugs Dampen the Cytokine and Antibody Response to SARS-CoV-2 Infection. *J. Virol.* **95**, (2021).
12. Jung, C. *et al.* Steroid use in elderly critically ill COVID-19 patients. *Eur. Respir. J.* 2100979 (2021) doi:10.1183/13993003.00979-2021.
13. Salama, C. *et al.* Tocilizumab in Patients Hospitalized with Covid-19 Pneumonia. *N. Engl. J. Med.* **384**, 20–30 (2021).
14. Mehta, P. *et al.* COVID-19: consider cytokine storm syndromes and immunosuppression. *Lancet* **395**, 1033–1034 (2020).
15. Combes, A. J. *et al.* Global absence and targeting of protective immune states in severe COVID-19. *Nat.* **2021 5917848** **591**, 124–130 (2021).
16. Wilk, A. J. *et al.* A single-cell atlas of the peripheral immune response in patients with severe COVID-19. *Nat. Med.* **2020 267** **26**, 1070–1076 (2020).
17. J, S.-S. *et al.* Severe COVID-19 Is Marked by a Dysregulated Myeloid Cell Compartment. *Cell* **182**, 1419–1440.e23 (2020).
18. ML, M. *et al.* A neutrophil activation signature predicts critical illness and mortality in COVID-19. *Blood Adv.* **5**, 1164–1177 (2021).
19. Wilk, A. J. *et al.* Multi-omic profiling reveals widespread dysregulation of innate immunity and hematopoiesis in COVID-19. *J. Exp. Med.* **218**, (2021).
20. Del Valle, D. M. *et al.* An inflammatory cytokine signature predicts COVID-19 severity and survival. *Nat. Med.* **26**, 1636–1643 (2020).
21. Overmyer, K. A. *et al.* Large-Scale Multi-omic Analysis of COVID-19 Severity. *Cell Syst.* **12**, 23–40.e7 (2021).
22. Park, J. *et al.* In-depth blood proteome profiling analysis revealed distinct functional

- characteristics of plasma proteins between severe and non-severe COVID-19 patients. *Sci. Rep.* **10**, (2020).
23. Lee, J. S. *et al.* Immunophenotyping of COVID-19 and influenza highlights the role of type I interferons in development of severe COVID-19. *Sci. Immunol.* **5**, (2020).
 24. Luo, X. *et al.* Prognostic Value of C-Reactive Protein in Patients With Coronavirus 2019. *Clin. Infect. Dis.* **71**, 2174–2179 (2020).
 25. Shu, T. *et al.* Plasma Proteomics Identify Biomarkers and Pathogenesis of COVID-19. *Immunity* **53**, 1108-1122.e5 (2020).
 26. Caricchio, R. *et al.* Preliminary predictive criteria for COVID-19 cytokine storm. *Ann. Rheum. Dis.* **80**, 88–95 (2021).
 27. Heller, R. A. *et al.* Prediction of survival odds in COVID-19 by zinc, age and selenoprotein P as composite biomarker. *Redox Biol.* **38**, (2021).
 28. Henry, B. M., De Oliveira, M. H. S., Benoit, S., Plebani, M. & Lippi, G. Hematologic, biochemical and immune biomarker abnormalities associated with severe illness and mortality in coronavirus disease 2019 (COVID-19): a meta-analysis. *Clin. Chem. Lab. Med.* **58**, 1021–1028 (2020).
 29. Fouladseresht, H. *et al.* Predictive monitoring and therapeutic immune biomarkers in the management of clinical complications of COVID-19. *Cytokine Growth Factor Rev.* **58**, 32–48 (2021).
 30. Majumder, J. & Minko, T. Recent Developments on Therapeutic and Diagnostic Approaches for COVID-19. *AAPS J.* **23**, (2021).
 31. Demichev, V. *et al.* A time-resolved proteomic and prognostic map of COVID-19. *Cell Syst.* **12**, 780-794.e7 (2021).
 32. T, H. *et al.* Elevated levels of IL-6 and CRP predict the need for mechanical ventilation in COVID-19. *J. Allergy Clin. Immunol.* **146**, 128-136.e4 (2020).
 33. Han, H. *et al.* Profiling serum cytokines in COVID-19 patients reveals IL-6 and IL-10 are disease severity predictors. (2020) doi:10.1080/22221751.2020.1770129.
 34. Silvin, A. *et al.* Elevated Calprotectin and Abnormal Myeloid Cell Subsets Discriminate Severe from Mild COVID-19. *Cell* **182**, 1401-1418.e18 (2020).
 35. Laing, A. G. *et al.* A dynamic COVID-19 immune signature includes associations with poor prognosis. *Nat. Med.* **2020 2610 26**, 1623–1635 (2020).
 36. Mazzoni, A. *et al.* Impaired immune cell cytotoxicity in severe COVID-19 is IL-6 dependent. *J. Clin. Invest.* **130**, 4694–4703 (2020).
 37. Y, Z. *et al.* Longitudinal COVID-19 profiling associates IL-1RA and IL-10 with disease severity and RANTES with mild disease. *JCI insight* **5**, (2020).
 38. Arunachalam, P. S. *et al.* Systems biological assessment of immunity to mild versus severe COVID-19 infection in humans. *Science (80-.)*. **369**, 1210–1220 (2020).
 39. Mahler, M., Meroni, P. L., Infantino, M., Buhler, K. A. & Fritzler, M. J. Circulating Calprotectin as a Biomarker of COVID-19 Severity. *Expert Rev. Clin. Immunol.* **17**, 431–443 (2021).
 40. Maucourant, C. *et al.* Natural killer cell immunotypes related to COVID-19 disease severity. *Sci. Immunol.* **5**, 6832 (2020).
 41. S, D. *et al.* Mucosal-Associated Invariant T (MAIT) Cells Are Highly Activated and Functionally Impaired in COVID-19 Patients. *Viruses* **13**, (2021).
 42. Bonnet, B. *et al.* Severe COVID-19 is characterized by the co-occurrence of moderate cytokine inflammation and severe monocyte dysregulation. *EBioMedicine* **73**, (2021).

43. Chevrier, S. *et al.* A distinct innate immune signature marks progression from mild to severe COVID-19. *Cell Reports Med.* **2**, 100166 (2021).
44. Wang, W. *et al.* High-dimensional immune profiling by mass cytometry revealed immunosuppression and dysfunction of immunity in COVID-19 patients. *Cell. Mol. Immunol.* **2020 176 17**, 650–652 (2020).
45. Peckham, H. *et al.* Male sex identified by global COVID-19 meta-analysis as a risk factor for death and ITU admission. *Nat. Commun.* **2020 111 11**, 1–10 (2020).
46. Guan, W. *et al.* Clinical Characteristics of Coronavirus Disease 2019 in China. *N. Engl. J. Med.* **382**, 1708–1720 (2020).
47. B, F. COVACTA trial raises questions about tocilizumab’s benefit in COVID-19. *Lancet. Rheumatol.* **2**, e592 (2020).
48. Ghanei, M. *et al.* The efficacy of corticosteroids therapy in patients with moderate to severe SARS-CoV-2 infection: a multicenter, randomized, open-label trial. *Respir. Res.* **22**, 1–14 (2021).
49. Liao, M. *et al.* Single-cell landscape of bronchoalveolar immune cells in patients with COVID-19. *Nat. Med.* **2020 266 26**, 842–844 (2020).
50. Melms, J. C. *et al.* A molecular single-cell lung atlas of lethal COVID-19. *Nat.* **2021 5957865 595**, 114–119 (2021).
51. Wauters, E. *et al.* Discriminating mild from critical COVID-19 by innate and adaptive immune single-cell profiling of bronchoalveolar lavages. *Cell Res.* **31**, 272–290 (2021).
52. Xu, G. *et al.* The differential immune responses to COVID-19 in peripheral and lung revealed by single-cell RNA sequencing. *Cell Discov.* **6**, (2020).
53. Stukas, S. *et al.* The Association of Inflammatory Cytokines in the Pulmonary Pathophysiology of Respiratory Failure in Critically Ill Patients With Coronavirus Disease 2019. *Crit. Care Explor.* **2**, e0203 (2020).

Table 1. Cohort clinical information

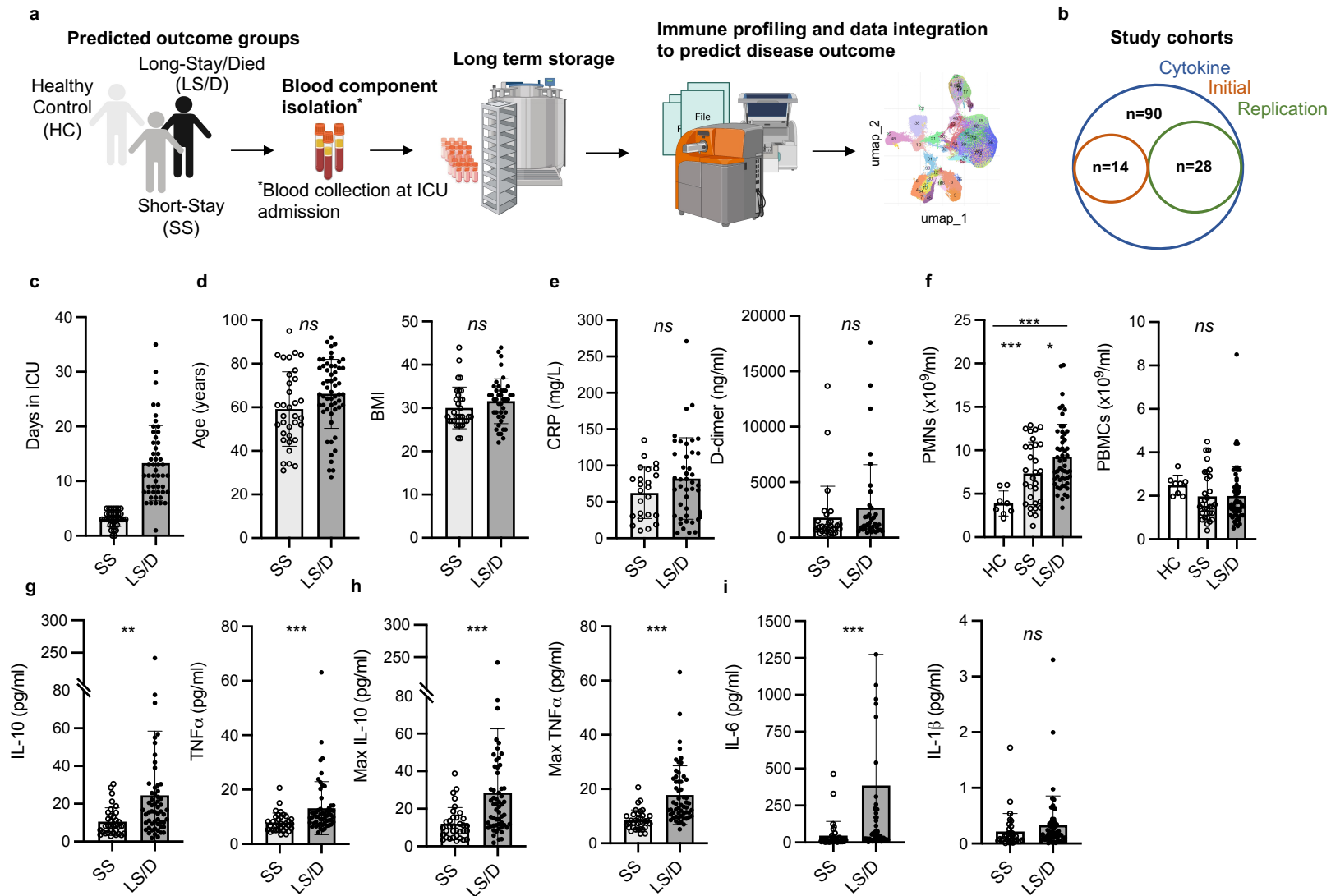
Characteristics	Healthy Controls (n = 8)	COVID-19 Patients (n=90) ¹
Age (mean years)	50.1	63.5
Sex (M:F)	5:3	56:34
Diagnosis	Asymptomatic/ healthy	SARS-COV-2 +
Collection timepoint (days)	NA	0-2 post admission
Severity	NA	ICU
BMI (mean)	NA	30.9
CRP (mean mg/L)	NA	75.6
D-dimer (mean ng/ml)	NA	3064.3
Length of stay (Short-Stay:Long-Stay/Died) ²	NA	34:56
Days in ICU (mean)	NA	9.3
Outcome (n; recovered:died)	NA	74:16
Mechanically ventilated (n, %)	NA	45, 60
PBMCs (mean 10 ⁹ /ml)	2.5	2.1
PMNs (mean 10 ⁹ /ml)	3.9	8.6

¹BMI, D-dimer, CRP and ventilation information was not available for 16/90 patients; calculations were adjusted accordingly.

²Short-Stay: <6 days; Long-Stay/Died: ≥ 6 days in ICU or Died.

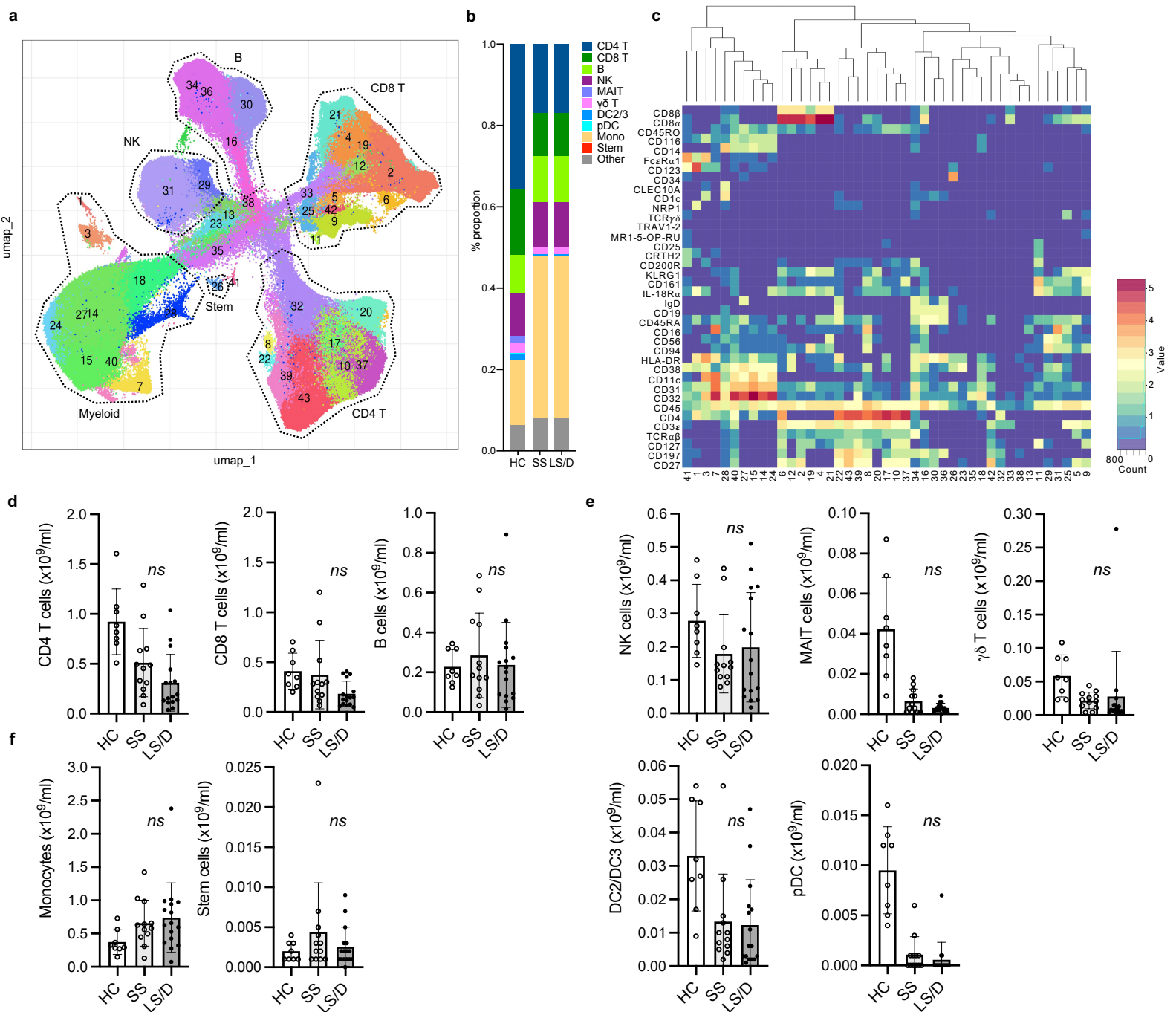
BMI: Body mass index; CRP: C-reactive protein; PBMCs: Peripheral blood mononuclear cells; PMNs: Polymorphonuclear leukocytes

Fig. 1: Patient cohort selection, characteristics and cytokine analyses.



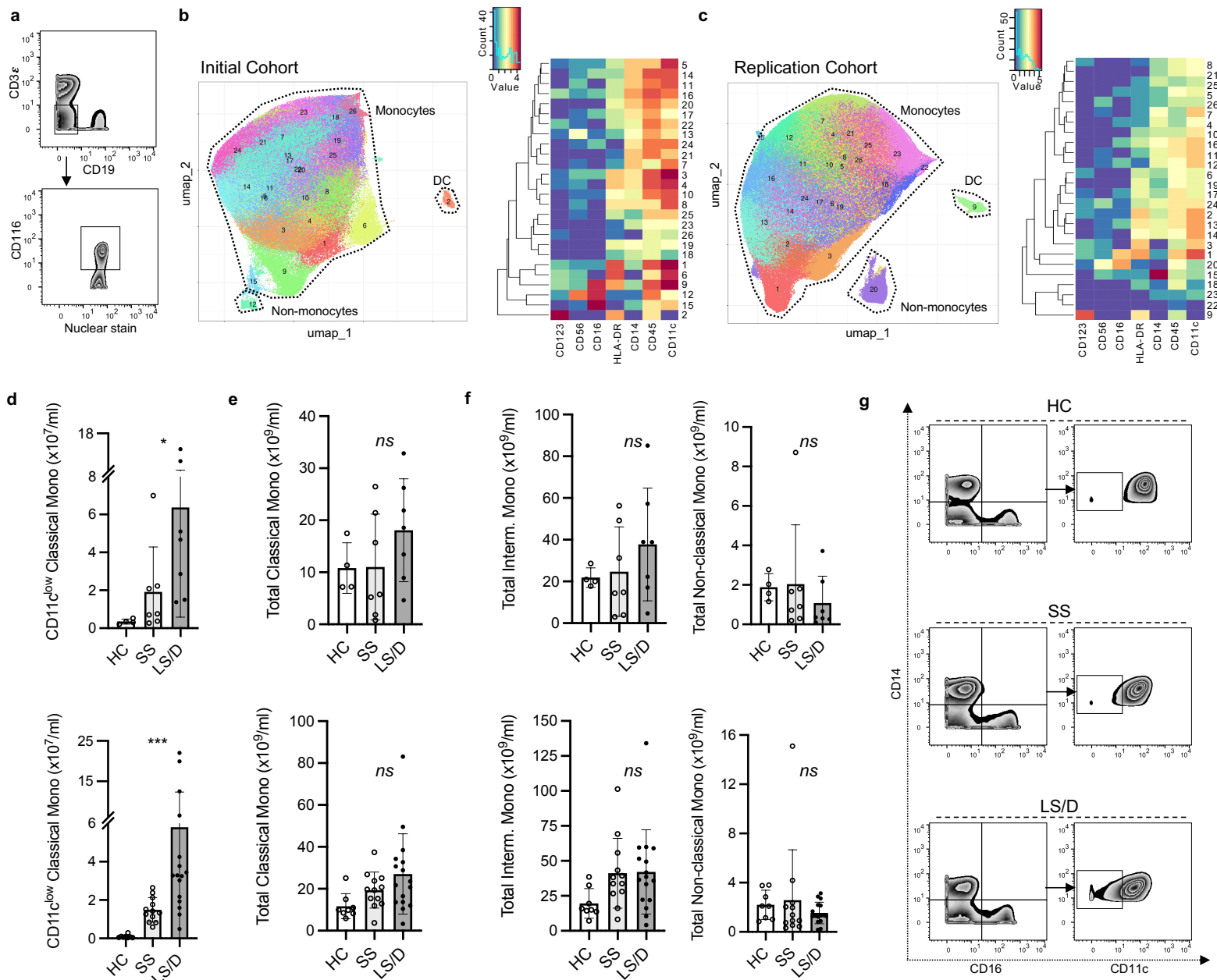
a, Experimental design overview: peripheral blood was collected from COVID-19 patients within 48h of ICU admission; immune cells and serum were isolated and stored followed by immune cell subset and cytokine analyses and clinical data integration. **b**, patient cohorts overview. **c**, patient outcome groups based on length of stay in ICU. (**d-e**), Patient age, body mass index (BMI), C-reactive protein (CRP) levels and D-dimer levels. **f**, Complete blood counts of patients and healthy controls. (**g-i**), Serum cytokine levels of IL-10, TNF α , maximum IL-10, maximum TNF α , IL-6 and IL-1 β . *, $p < 0.05$; **, $p < 0.01$; ***, $p < 0.001$; ns, $p \geq 0.05$ by two-tailed, two-sample unequal variance Student's t-Test.

Fig. 2: Major PBMC subsets fail to identify Long-Stay/Died patients in the Replication Cohort.



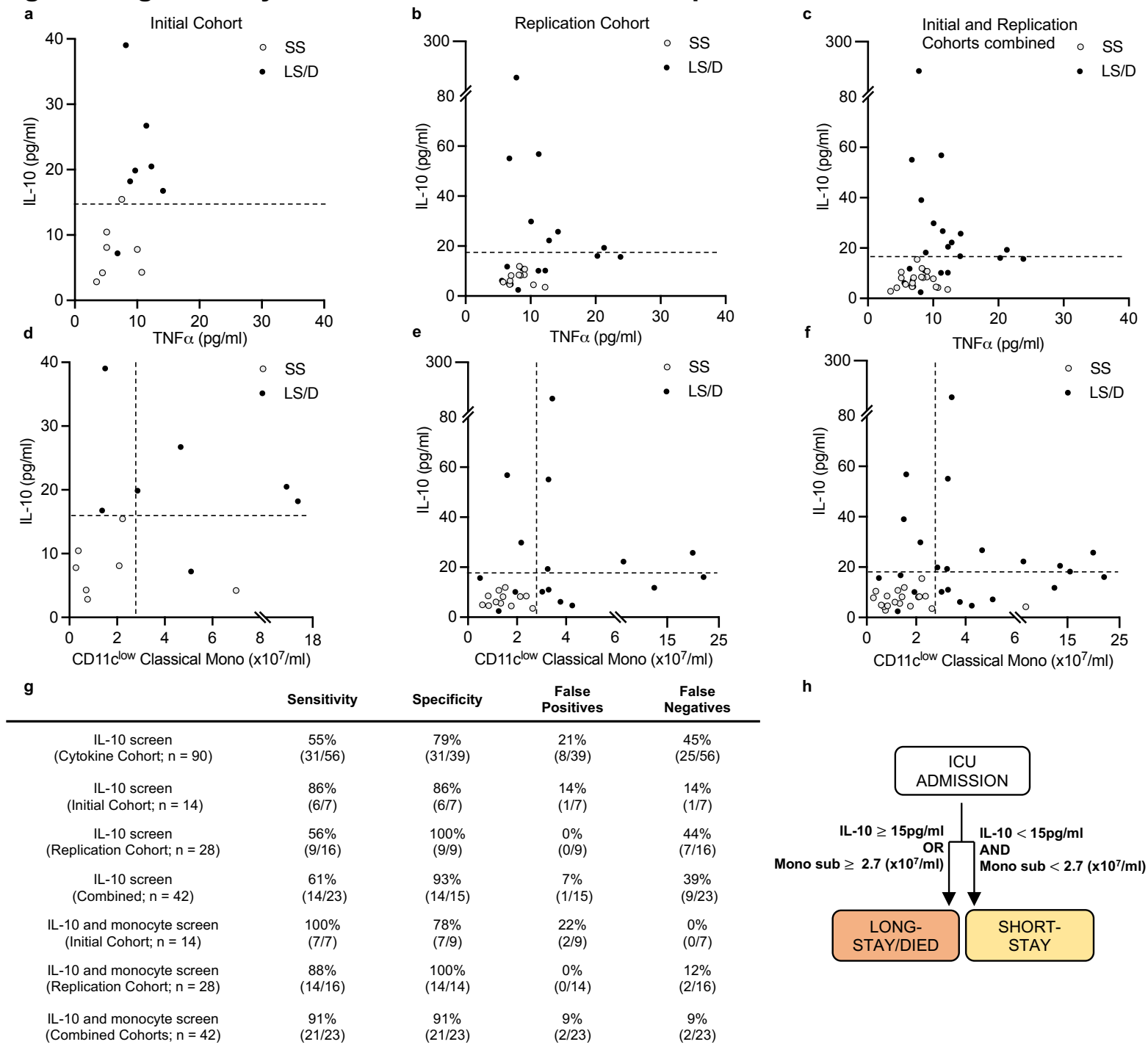
a, UMAP projection of ungated CyTOF-derived data from the replication cohort (n=28). **b**, proportion of immune cell subsets in Healthy Controls (HC), Short-Stay (SS) and Long-Stay/Died (LS/D) patient outcome groups **c**, Mean marker expression heatmap of clusters shown in **a**. **d**, Absolute counts of adaptive PBMC subsets (CD4 T, CD8 T, B), **e**, innate and unconventional subsets (NK, MAIT, $\gamma\delta$ T, pDC, DC2/3), **f**, monocytes and stem cells. *, $p < 0.05$; **, $p < 0.01$; ***, $p < 0.001$; ns, $p \geq 0.05$ by two-tailed, two-sample unequal variance Student's t-Test.

Fig. 3: CD11c^{low} Classical Monocytes are predictive of clinical outcome.



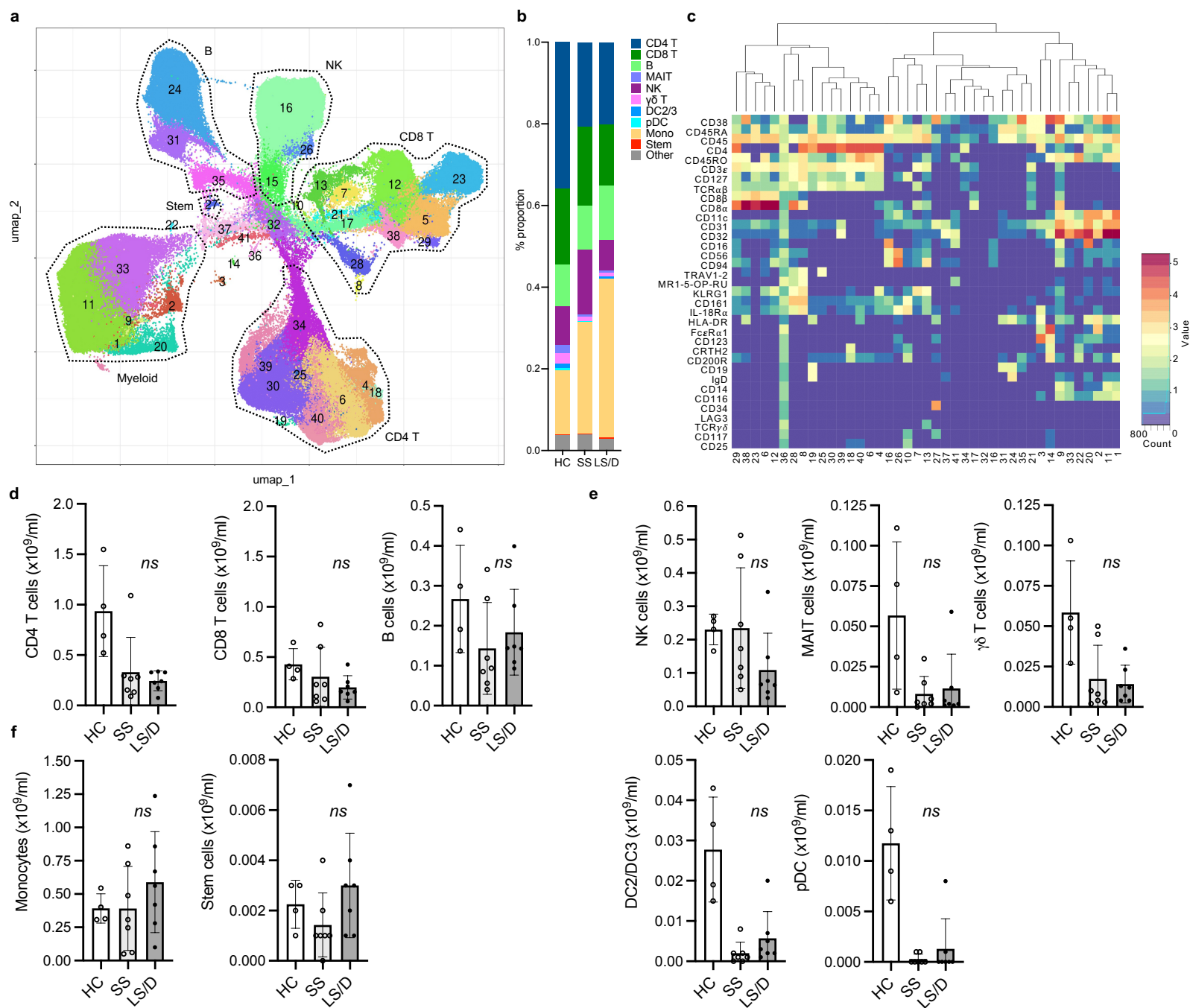
a, Representative gating of CD116⁺CD3⁻CD19⁻ cells. **b**, Initial Cohort UMAP projections of CD116⁺CD3⁻CD19⁻ gated cells (all samples combined; limited clustering channels) and mean marker expression heatmap. **c**, same as in **b** but for the Replication Cohort. **d**, Initial (top) and Replication Cohorts (bottom) absolute counts of monocyte subset predictive of clinical outcome. **e-f**, Absolute counts of non-significant monocyte subset identified based on gated clustering (top row: Initial Cohort, bottom row: Replication Cohort). **g**, Manual gating strategy to view predictive monocyte subset. *, p < 0.05; **, p < 0.01; ***, p < 0.001; ns, p ≥ 0.05 by two-tailed, two-sample unequal variance Student's t-Test.

Fig. 4: Prognostic cytokine and cellular biomarkers predict clinical outcome.



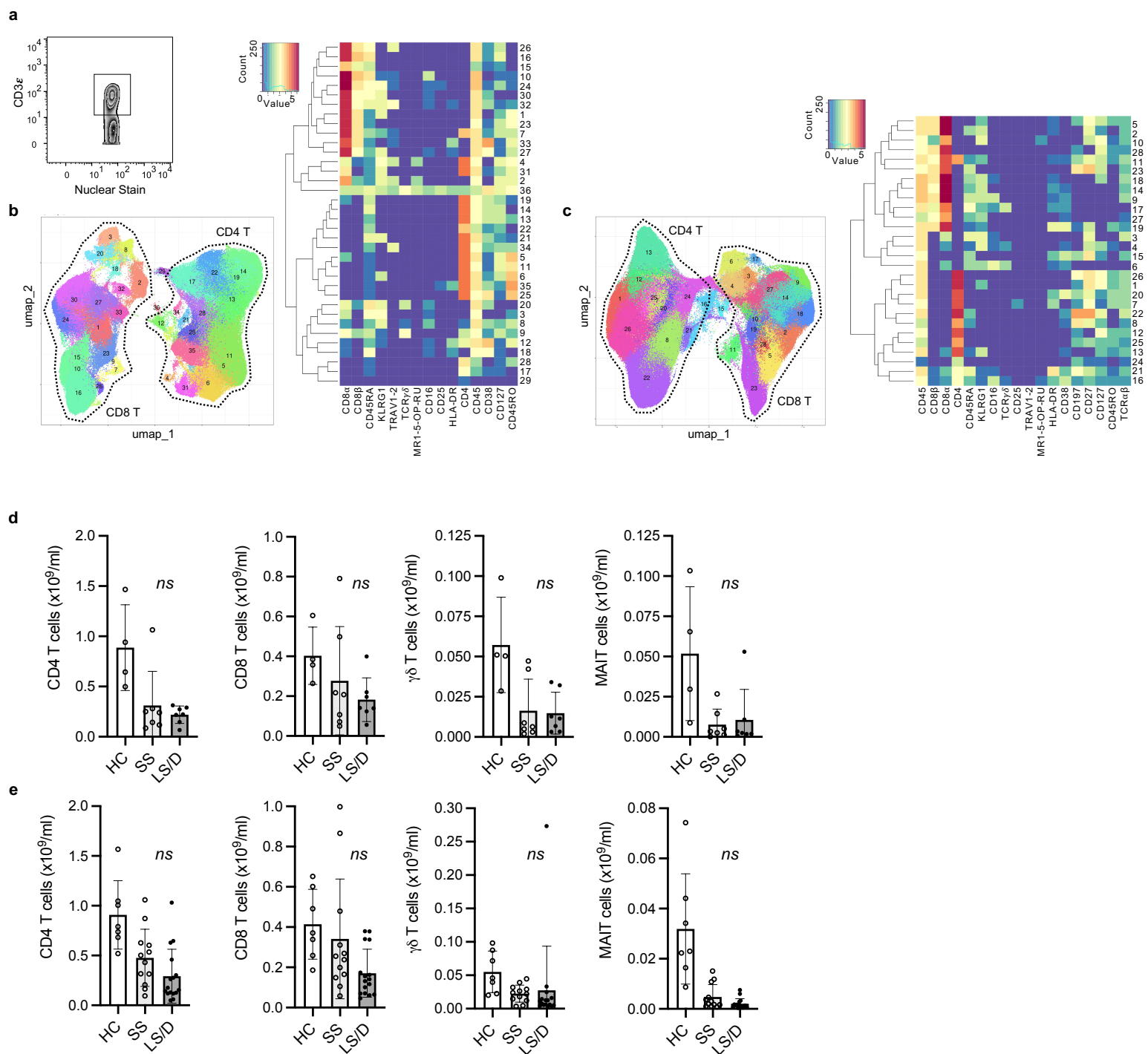
a-c, Cytokine levels scatter plots of Initial (left), Replication (middle) and combined Cohorts (right) with dashed lines at cut-off value of 15pg/ml for serum IL-10. **d-f**, Cytokine and cellular levels scatter plots for Initial (left) Replication (middle) and combined cohorts (right) with dashed lines at cut-off values of 15pg/ml and 2.7 (x10⁷/ml) of serum IL-10 and CD11c^{low} classical monocytes respectively. **g**, Sensitivity and specificity calculations for each screen and cohort. **h**, Prognostic patient screening chart based on serum IL-10 and CD11c^{low} monocyte subset measurement. *, p < 0.05; **, p < 0.01; ***, p < 0.001; ns, p ≥ 0.05 by two-tailed, two-sample unequal variance Student's t-Test and R² by two-tailed Pearson correlation with 95% confidence interval.

Fig. S1: Major PBMC subsets fail to identify Long-Stay/Died patients in the Initial Cohort.



a, UMAP projection of un gated CyTOF-derived data from the Initial cohort (n=14). **b**, proportion of immune cell subsets in Healthy Controls (HC), Short-Stay (SS) and Long-Stay/Died (LS/D) patient outcome groups **c**, Mean marker expression heatmap of clusters shown in **a**. **d**, Absolute counts of adaptive PBMC subsets (CD4 T, CD8 T, B), **e**, innate and unconventional subsets (NK, MAIT, $\gamma\delta$ T, pDC, DC2/3), **f**, monocytes and stem cells. *, $p < 0.05$; **, $p < 0.01$; ***, $p < 0.001$; ns, $p \geq 0.05$ by two-tailed, two-sample unequal variance Student's t-Test.

Fig. S2: T cell subsets fail to identify Long-Stay/Died patients.



a, Representative gating of CD3⁺ cells. **b**, Initial Cohort UMAP projections of CD3⁺ gated cells (all samples combined; limited clustering channels) and mean marker expression heatmap. **c**, same as in **b** but for the Replication Cohort. **d**, Initial Cohort absolute counts of T cell subsets identified based on gated clustering. **e**, same as in **d** but for the Replication Cohort. *, $p < 0.05$; **, $p < 0.01$; ***, $p < 0.001$; ns, $p \geq 0.05$ by two-tailed, two-sample unequal variance Student's t-Test.

Table S1. List of CyTOF antibodies

Antibody/Tetramer	Metal/Fluorophore*	Clone	Company	Used in Cohort
CD1c	151Eu	L161	Biolegend	Replication
CD3 ϵ	143Nd	OKT3	Biolegend	both
CD4	174Yb	SK3	Biolegend	both
CD8 α	168Er	SK1	Biolegend	both
CD8 β	141Pr	SIDI8BEE	eBioscience	both
CD11c	147Sm	Bu15	Biolegend	both
CD14	153Eu	M5E2	Biolegend	both
CD16	158Gd	3G8	Biolegend	both
CD19	142Nd	HIB19	Biolegend	both
CD25	169Tm	BC96	Biolegend	both
CD27	175Lu	O323	Biolegend	Replication
CD31	145Nd	WM59	Biolegend	both
CD32	160Gd	IV.3	Stemcell Technologies	both
CD34	156Gd	581	Biolegend	both
CD38	106Cd	HIT2	Biolegend	both
CD45	89Y	HI30	Biolegend	both
CD45RA	110Cd	HI100	Biolegend	both
CD45RO	112Cd	UCHL1	Biolegend	both
CD56	148Nd	NCAM16.2	BD Bioscience	both
CD94 (NKG2C)	161Dy	DX22	Biolegend	both
CD116	150Nd	4H1	Biolegend	both
CD117	171Yb	104D2	Biolegend	Initial
CD123	164Dy	6H6	Biolegend	both
CD127	165Ho	A019D5	Biolegend	both
CD161	159Tb	HP-3G10	Biolegend	both
CD197/CCR7	171Dy	G043H7	Biolegend	Replication
CD200R	173Yb	0X-108	BD Bioscience	both
CD294 (CRTH2)	163Dy	BM16	Biolegend	both
CD301 (CLEC10A)	154Sm	H037G3	Biolegend	Replication
CD304 (NRP1)	172Yb	12C2	Biolegend	Replication
Fc ϵ R α 1	176Yb	AER-37	Biolegend	both
HLA-DR	170Er	L243	Biolegend	both
IgD	116Cd	IA6-2	Biolegend	both
IL-18R α	162Dy	H44	Biolegend	both
KLRG1	144Nd	SA231A2	Biolegend	both
LAG3	175Lu	11C3C65	Biolegend	Initial
TCR $\alpha\beta$	155Gd	T10B9.1A-31	BD Bioscience	both
TCR $\gamma\delta$	152Sm	B1	Biolegend	both
TRAV1-2	115Ln	3C10	Biolegend	both
Anti-APC (Secondary)	149Sm	APC003	Biolegend	both
MR1-5-OP-RU (Primary)	APC	NA	NIH Tetramer Facility	both